

Exploring the Photocatalytic Properties and the Long-Lifetime Chemosensor Ability of $\text{Cl}_2[\text{Ru}(\text{Bpy})_2\text{L}]$ ($\text{L} = 2,5,8,11,14\text{-Pentaaza[15]-}2,2'\text{-bipyridilophane}$)

Carlos Lodeiro,[†] Fernando Pina,^{*,†} A. Jorge Parola,[†] Andrea Bencini,[‡] Antonio Bianchi,^{*,‡} Carla Bazzicalupi,[‡] Samuele Ciattini,[‡] Claudia Giorgi,[‡] Andrea Masotti,[‡] Barbara Valtancoli,[‡] and J. Seixas de Melo[§]

Departamento de Química, Centro de Química-Fina e Biotecnologia, Faculdade de Ciências e Tecnologia, Universidade Nova de Lisboa, Quinta da Torre 2825 Monte de Caparica, Portugal, Department of Chemistry, University of Florence, Via della Lastruccia 3, 50019 Sesto Fiorentino, Florence, Italy, Departamento de Química, Universidade de Coimbra, 3049 Coimbra, Portugal

Received May 17, 2001

In this work a new water-soluble long-lifetime chemosensor, containing a polyamine unit connected to a complexed Ru(II) metal center, is described. Its crystal structure has been characterized by X-ray analysis. The polyamine macrocyclic unit is capable of anchoring cationic or anionic substrates, according to its protonation state. Examples of electron transfer involving the ruthenium complex core and the bound substrate are presented. The photocatalytic ability of such a system is illustrated by the oxidation of iodide to iodine promoted by light absorption at 436 nm.

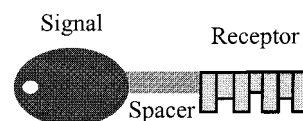
Introduction

In recent years we have developed a series of water-soluble chemosensors based on polyamine receptors exhibiting ambidentate properties. They possess the capability of coordinating metal cations, when enough free (unprotonated) amine groups are available, or anions, when the number of protonated amino groups is sufficiently high.¹

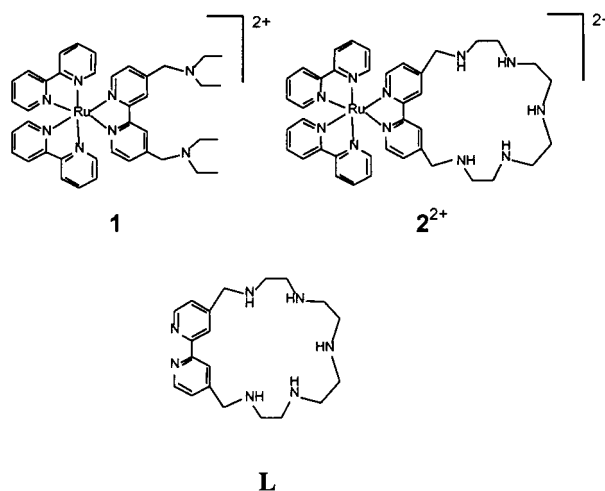
In essence, three basic units make up these chemosensors, each one performing a precise function: (i) a receptor unit, (ii) a signaling unit, and (iii) a spacer (Scheme 1). The receptor unit plays the role of recognizing and reversibly binding a given target substrate. The signaling unit, in turn, must be capable of either producing a signal or significantly altering its intensity following the binding of the substrate, preferably without changing other photochemical properties of the chemosensor. Finally, the third unit, the spacer, links binding and signaling units controlling their mutual separation and geometric arrangement.

The majority of the reported chemosensors^{1–3} possess a signaling unit sensitive to the changes of luminescence intensity, leading to chelation enhancement of the fluorescence, CHEF, or chelation enhancement of the quenching, CHEQ.² On the other hand, the particular usefulness of *lifetime based sensing*

Scheme 1



systems has been pointed out, essentially because they do not depend on probe concentration and remain unaffected by the photobleaching or washout of the probe.⁴ Following this line of thought, Lakowicz and co-workers^{4b} developed a study on compound **1**, acting as a long-lifetime metal–ligand pH probe. To improve both the preorganization and the binding ability of the system toward cations and anions, we have carried out the synthesis of compound $\text{Ru}(\text{bpy})_2\text{L}^{2+}$ (**2²⁺**), characterized by a



large macrocyclic receptor unit containing five amine groups.

* Corresponding authors. E-mail: fjp@dq.fct.unl.pt. E-mail: bianchi@chim1.unifi.it.

[†] Universidade Nova de Lisboa.

[‡] University of Florence.

[§] Universidade de Coimbra.

- (1) (a) Pina, F.; Bernardo, M. A.; García-España, E. *Eur. J. Inorg. Chem.* **2000**, 2143. (b) Bazzicalupi, C.; Bencini, A.; Bianchi, A.; Giorgi, C.; Fusi, V.; Valtancoli, B.; Bernardo, M. A.; Pina, F. *Inorg. Chem.* **1999**, 38, 3806.
- (2) (a) Czarnik, A. W. *Acc. Chem. Res.* **1994**, 27, 302. (b) Czarnik, A. W. *Fluorescent Chemosensors for Ion and Molecule Recognition*; American Chemical Society: Washington, DC, 1992.
- (3) (a) Bissel, R. A.; De Silva, A. P.; Gunaratne, H. Q. N.; Lynch, P. L. M.; Maguire, G. E. M.; Sandanayake, K. R. A. S. *Chem. Soc. Rev.* **1992**, 187. (b) De Silva, A. P.; Gunaratne, H. Q. N.; Gunnlaugsson, T.; Huxley, A. J. M.; McCoy, C. P.; Rademacher, J. T.; Rice, T. E. *Chem. Rev.* **1997**, 97, 1515.

- (4) (a) *Probe design and chemical sensing*; Topics in Fluorescence Spectroscopy 4; Lakowicz, J. R., Ed.; Plenum Press: New York, 1994. (b) Murtaza, Z.; Chang, Q.; Rao, G.; Lin, H.; Lakowicz, J. R. *Anal. Biochem.* **1997**, 247, 216.

Ligands containing two amino groups, similar to compound **1**, have been previously described by Grigg et al. as fluorescence intensity based pH sensors.^{5a} Other fluorescence intensity based receptors containing a cyclam macrocycle attached to a Ru-(bpy)₃²⁺ unit were also reported to bind metal cations.^{5b,6} On the other hand, Beer and co-workers have synthesized and studied analogous ligands containing amidic functions.⁷ These receptors give rise to selective anion recognition in organic solvents, mostly due to anion–receptor hydrogen bonding, functioning as sensory reagents for anions.⁷ Binding and sensing of phosphate anions, however, were also achieved by the same author in acidic aqueous solutions, by using Ru^{II}(bpy)₃-based receptors containing two diamine sidearms.⁸ Nocera et al. used Ru^{II}(tmbpy)₃ (tmbpy = 4-methyl-2,2'-dipyridine) derivatives, containing a carboxylate or a guanidinium function, as receptors for amidinium- or carboxylate-modified 3,5-dinitrobenzene, respectively, to investigate photoinduced electron transfer within donor–(salt bridge)–acceptor complexes.⁹ Photoinduced electron and energy transfer processes between nucleobases were also studied in nonaqueous solvents by Sessler and Harriman, by using nucleobase-substituted porphyrins designed to form hydrogen-bonded assemblies through Watson–Crick nucleobase-pairing interactions.¹⁰

Compounds containing the new receptor **2**²⁺ are generally soluble in water, thus allowing us to develop a detailed study, in aqueous solution, of its ligational and photochemical properties, including stability of cation and anion complexes, steady-state and time-resolved fluorescence as a function of pH, and quenching with several metal cations and anions. The ability of this chemosensor in promoting the oxidation of iodide to iodine by dioxygen was also investigated.

Experimental Section

Materials. All materials were of reagent grade and used without further purification. The synthesis of 4,4'-(2,5,8,11,14-pentaaza[15]-2,2'-bipyridilophane (**L**) was described in a previous paper.¹¹

Synthesis of (H₂)Cl₇. In 5 mL of ethylene glycol 100.0 mg (0.115 mmol) of L·6HBr·H₂O and 62.6 mg (0.120 mmol) of Ru(bpy)₂Cl₂·2H₂O were dissolved. The mixture was heated in a microwave oven (500 W) for 30 s, which led to a color change from violet to deep

Table 1. Crystal Data and Structure Refinement for (H₂)₂(ClO₄)₅·H₂O

empirical formula	C ₄₀ H ₅₂ Cl ₅ N ₁₁ O ₂₁ Ru
formula weight	1301.25
temperature	298 K
wavelength	0.710 69 Å
crystal system, space group	monoclinic, P2 ₁ /c
a	18.380(4) Å
b	13.147(5) Å
c	22.931(7) Å
β	109.37(2)°
volume	5227(3) Å ³
Z, calculated density	4, 1.653 mg/m ³
absorption coefficient	0.644 mm ⁻¹
scan mode	θ–2θ
θ range for data collection	2.53°–24.05°
reflections collected/unique	9593/5235 [R(int) = 0.0884]
observed reflections [I > 2σ(I)]	2721
data/restraints/parameters	5235/0/512
goodness of fit on R ²	1.003
final R indices [I > 2σ(I)]	R1 = 0.0558, wR2 = 0.1336
R indices (all data)	R1 = 0.1657, wR2 = 0.1677

orange, and then allowed to cool for a while. The mixture was heated for two more 30 s periods. The solvent was removed by distillation at low pressure, and the residue was dissolved in 6 M HCl. Acetone was added to precipitate the product as a red-orange solid that was collected, washed with acetone until neutrality, and finally washed with ether. It can be recrystallized from methanol/acetonitrile/ether or from acidic water/acetone, the latter leading to better results. Anal. Found: C, 46.44; H, 5.12; N, 14.98. Calcd. for C₄₀H₅₂N₁₁Cl₇Ru: C, 46.37; H, 5.06, 14.87. The yield was about 80%. ¹H NMR (D₂O + DCl, pH < 2, 400 MHz, Bruker ARX-400): δ/ppm 8.584 (s, 2H, L, 3H + 3'H), 8.299 (d, J = 8.2 Hz, 4H, bpy, 3H + 3'H), 7.815 (m, 4H, bpy, 4H + 4'H), 7.679 (d, J = 5.8 Hz, 2H, L, 6H + 6'H), 7.556 (2d, J = 5.4 Hz, 4H, bpy, 6H + 6'H), 7.153 (m, 6H, L, 5H + 5'H, bpy, 5H + 5'H), 4.387 (m, 4H, L, pyCH₂N), 3.547 (m, 16H, NCH₂CH₂N).

Crystals of [Ru(bpy)₂H₃L](ClO₄)₅·H₂O suitable for X-ray analysis were obtained by slow evaporation at room temperature of a water–acetone 1:1 (v/v) solution of [Ru(bpy)₂H₃L]Cl₇ after addition of excess solid sodium perchlorate. The composition of the compounds was determined by X-ray analysis.

X-ray Structure Determination of Compound (H₂)₂(ClO₄)₅·H₂O.

Crystal and data collection parameters are summarized in Table 1. Intensity data were corrected for Lorentz and polarization effects, and an empirical absorption correction was applied (psi-scan). The structure was solved by direct methods of SIR97¹² program. All the non-hydrogen atoms, except the carbon atoms, were anisotropically refined, while the hydrogen atoms were introduced in calculated position and their coordinates and thermal parameters refined according to the linked carbon atom. Refinement was performed by the full-matrix least-squares method (SHELXL-97).¹³

Potentiometric Measurements. All pH-metric measurements (pH = –log [H⁺]) employed for the determination of protonation and complexation (metal cations, anions) constants were carried out in 0.10 M Me₄NCl solutions at 298.1 ± 0.10 K, by using the equipment and the methodology that have been already described.¹⁴ The combined Ingold 405 S7/120 electrode was calibrated as a hydrogen concentration probe by titrating known amounts of HCl with CO₂-free NaOH solutions and determining the equivalent point by Gran's method,¹⁵ which allows one to determine the standard potential E^o and the ionic product of water (pK_w = 13.83(1) at 298.1 K in 0.10 M Me₄NCl). At least three measurements (about 100 data points each one) were performed for each system in the pH ranges 2.5–11 (2.5–10 in the case of anion complexation). In all experiments the ligand concentration [L] was about

- (5) (a) Grigg, R.; Norbert, W. D. *J. Chem. Soc. Chem. Commun.* **1992**, 1300. (b) Kimura, E.; Wada, S.; Shionoya, M.; Takahashi, T.; Litaka, Y. *J. Chem. Soc. Chem. Commun.* **1990**, 397.
- (6) (a) Rawle, S. C.; Moore, P.; Alcock, N. W. *J. Chem. Soc., Chem. Commun.* **1992**, 684. (b) Alcock, N. W.; Clarke, A. J.; Errington, W.; Josceanu, A. M.; Moore, P.; Rawle, S. C.; Sheldon, P.; Smith, S. M.; Turonek, M. *Supramol. Chem.* **1996**, *6*, 281, and references therein.
- (7) (a) Szemes, F.; Heseck, D.; Chen, Z.; Dent, S. W.; Drew, M. G. B.; Goulden, A. J.; Graydon, A. R.; Grieve, A.; Mortimer, R. J.; Wear, T.; Weightman, J. S.; Beer, P. D. *Inorg. Chem.* **1996**, *35*, 5868. (b) Beer, P. D.; Szemes, F.; Balzani, V.; Salà, C. M.; Drew, M. G. B.; Dent, S. W.; Maestri, M. *J. Am. Chem. Soc.* **1997**, *119*, 11864. (c) Beer, P. D. *Acc. Chem. Res.* **1998**, *31*, 71. (d) Beer, P. D.; Gale, P. A. *Angew. Chem., Int. Ed.* **2001**, *40*, 486.
- (8) Beer, P. D.; Cadman, J. *New J. Chem.* **1999**, *23*, 347.
- (9) (a) Turró, C.; Chang, C. K.; Leroy, G. E.; Cukier, R. I.; Nocera, D. G. *J. Am. Chem. Soc.* **1992**, *114*, 4013. (b) Roberts, J. A.; Kirby, J. P.; Nocera, D. G. *J. Am. Chem. Soc.* **1995**, *117*, 8051. (c) Deng, Y.; Roberts, J. A.; Peng, S. M.; Chang, C. K.; Nocera, D. G. *Angew. Chem., Int. Ed. Engl.* **1997**, *36*, 2124. (d) Kirby, J. P.; Roberts, J. A.; Nocera, D. G. *J. Am. Chem. Soc.* **1997**, *119*, 9230.
- (10) (a) Harriman, A.; Magda, D. J.; Sessler, J. L. *J. Phys. Chem. B* **1991**, *95*, 1530. (b) Harriman, A.; Magda, D. J.; Sessler, J. L. *J. Chem. Soc., Chem. Commun.* **1991**, 345. (c) Harriman, A.; Kubo, Y.; Sessler, J. L. *J. Am. Chem. Soc.* **1992**, *114*, 388. (d) Harriman, A.; Bing, W.; Sessler, J. L. *J. Am. Chem. Soc.* **1993**, *115*, 10418. (e) Harriman, A.; Bing, W.; Sessler, J. L. *J. Am. Chem. Soc.* **1995**, *117*, 704.
- (11) Lodeiro, C.; Parola, A. J.; Pina, F.; Bazzicalupi, C.; Bencini, A.; Bianchi, A.; Giorgi, C.; Masotti, A.; Valtancoli, B. *Inorg. Chem.* **2001**, *40*, 2968.

- (12) Altomare, A.; Burla, M. C.; Camalli, M.; Casciaro, G. L.; Giacovazzo, C.; Guagliardi, A.; Moliterni, A. G. G.; Polidori, G.; Spagna, R. *J. Appl. Crystallogr.* **1999**, *32*, 115.
- (13) Sheldrick, G. M. *SHELXL97*; University of Göttingen, Germany, 1997.
- (14) Bianchi, A.; Bologni, L.; Dapporto, P.; Micheloni, M.; Paoletti, P. *Inorg. Chem.* **1984**, *23*, 1201.
- (15) Gran, G. *Analyst (London)* **1952**, *77*, 661.

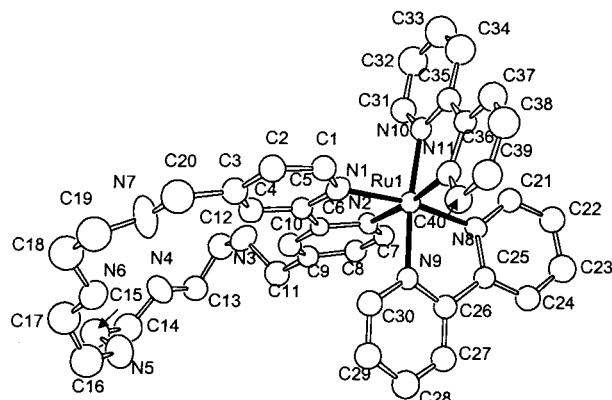


Figure 1. Crystal structure of $\text{H}_3\text{2}^{5+}$.

1×10^{-3} M. In Zn(II) complexation experiments, the metal ion concentration was $[\text{Zn}(\text{II})] = 0.8[\text{L}]$, while in the case of Cu(II) complexation it was varied from $[\text{Cu}(\text{II})] = 0.8[\text{L}]$ to $[\text{Cu}(\text{II})] = 1.8[\text{L}]$. In anion complexation experiments the concentration of anion $[\text{A}]$ was varied from $[\text{A}] = [\text{L}]$ to $[\text{A}] = 2[\text{L}]$. The computer program HYPERQUAD¹⁶ was used to calculate the equilibrium constants from emf data.

Electronic Absorption and Emission Measurements. Absorption spectra were recorded by means of a Perkin-Elmer Lambda 6 spectrophotometer, while fluorescence emission was recorded on a SPEX F111 Fluorolog spectrofluorimeter. Fluorescence lifetimes were measured by using two different equipment. One was a TCSPC apparatus consisting of a IBH 5000 coaxial flash lamp filled with N_2 as excitation source, a Philips XP2020Q photomultiplier, with wavelength selected with Jobin-Ivon H20 monochromator, and Canberra instruments time-to-amplitude converter and multichannel analyzer. Alternate measurements (1000 counts per cycle at the maximum) of the pulse profile at 356 nm and the sample emission were performed until $(1-2) \times 10^4$ counts at the maximum were reached. The luminescence decays were analyzed using the method of modulating functions of G. Striker with automatic correction for the photomultiplier "wavelength shift".¹⁷ The second one was an Applied Photophysics laser flash photolysis equipment pumped by a Nd:YAG laser (Spectra Physics) with excitation wavelength 355 or 266 nm.¹⁸ We have used the emission mode to obtain the luminescence decays. First-order kinetics was observed for the luminescence decays. In all experiments the concentration of the receptor was about 1×10^{-5} M; HCl and NMe_4OH solutions were used to adjust the pH, measured by means of a Metrohm 713 pH meter.

The solutions used for the emission studies were not degassed and therefore were used with normal concentrations of O_2 present in the solvents, i.e., $\approx 10^{-3}$ M.

Results and Discussion

Crystal Structure of $(\text{H}_3\text{2})(\text{ClO}_4)_5 \cdot \text{H}_2\text{O}$. The molecular structure consists of $(\text{H}_3\text{2})^{5+}$ cations, perchlorate anions, and water solvent molecules. Figure 1 shows an ORTEP¹⁹ drawing of the cation with atom labeling.

The ligand **L** behaves in this compound as a ditopic receptor, involving the aromatic nitrogens of its dipyrindine moiety in metal coordination outside the macrocyclic cavity and the aliphatic chain in proton binding.

The coordination geometry around Ru(II) can be described as a slightly distorted octahedron, where the N1–N8, N2–N11, and N9–N10 pairs of atoms define opposite vertices of the

Table 2. Protonation Constants of 2^{2+} Determined in 0.10 M Me_4NCl at 298.1 ± 0.1 K

reaction	$\log K$
$\text{H}^+ + \text{2}^{2+} = \text{H2}^{3+}$	8.92(5) ^a
$\text{H2}^{3+} + \text{H}^+ = \text{H2}^{4+}$	8.10(5)
$\text{H2}^{4+} + \text{H}^+ = \text{H3}^{5+}$	5.54(6)
$\text{H3}^{5+} + \text{H}^+ = \text{H4}^{6+}$	3.97(6)
$\text{H4}^{6+} + \text{H}^+ = \text{H5}^{7+}$	3.03(6)

^a Values in parentheses are standard deviations in the last significant figure.

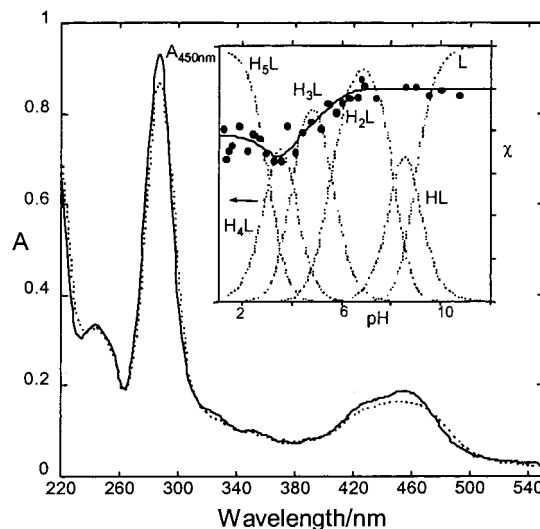


Figure 2. Absorption spectra of compound 2^{2+} (**L**), 1.33×10^{-5} M, at two representative pH values: (—) pH 7.33, (···) pH 4.09. Inset: fitting of the absorption followed at 450 nm, together with the representation of the mole fraction (χ) distribution of the protonated species. Charges omitted in species labels.

polyhedron. Such coordination environment is quite similar to the environments observed in $[\text{Ru}(\text{bpy})_3]^{2+}$ and other similar complexes containing a dipyrindine group integrated into a macrocyclic ring.^{7,20}

The overall conformation of **L** is slightly bent, as evidenced by the dihedral angle of $142.6(2)^\circ$ between the mean planes defined by the aromatic and aliphatic **L** moieties.

The crystal packing is characterized by $(\text{H}_3\text{2})^{5+}$ units, interacting with each other via both face-to-face and edge-to-face π -stackings²¹ between the aromatic units. The complexes are pillared, forming columns developing along the y axis. A detailed description of the crystal packing is reported within the Supporting Information.

Protonation. The protonation constants of 2^{2+} determined in 0.10 M Me_4NCl at 298.1 ± 0.1 K are listed in Table 2, while the distribution curves of the protonated species are shown in the inset of Figure 2. As can be seen, on lowering the pH, the compound starts binding protons at about pH 10 and is almost completely protonated at pH 2, where the $\text{H}_5\text{2}^{7+}$ species is present in more than 90%. The protonation constants are consistent with the protonation pattern expected for a polyamine macrocycle,²² although the compound displays a lower basicity, in each protonation stage, than the free macrocycle **L**, due to the presence in 2^{2+} of a lower number of amine groups available for protonation and to the electrostatic repulsion generated by

(16) Gans, P.; Sabatini, A.; Vacca, A. *Talanta* **1996**, *43*, 1739.
 (17) Stricker, G.; Subramaniam, V.; Seidel, C. A. M.; Volkmer, A. *J. Phys. Chem. B* **1999**, *103*, 8612.
 (18) Seixas de Melo, J.; Elisei, F.; Gartner, C.; Aloisi, G.; Becker, R. S. *J. Phys. Chem. A* **2000**, *104*, 6907.
 (19) Farrugia, L. J. *ORTEP-3* Windows version 1.01 beta; Department of Chemistry: University of Glasgow, 1997.

(20) Rillema, D. P.; Jones, D. S.; Woods, C.; Levy, H. A. *Inorg. Chem.* **1992**, *31*, 2935.
 (21) Janiak, C. *J. Chem. Soc., Dalton Trans.* **2000**, 3885.
 (22) Bencini, A.; Bianchi, A.; Garcia-España, E.; Micheloni, M.; Ramirez, J. A. *Coord. Chem. Rev.* **1999**, *188*, 97.

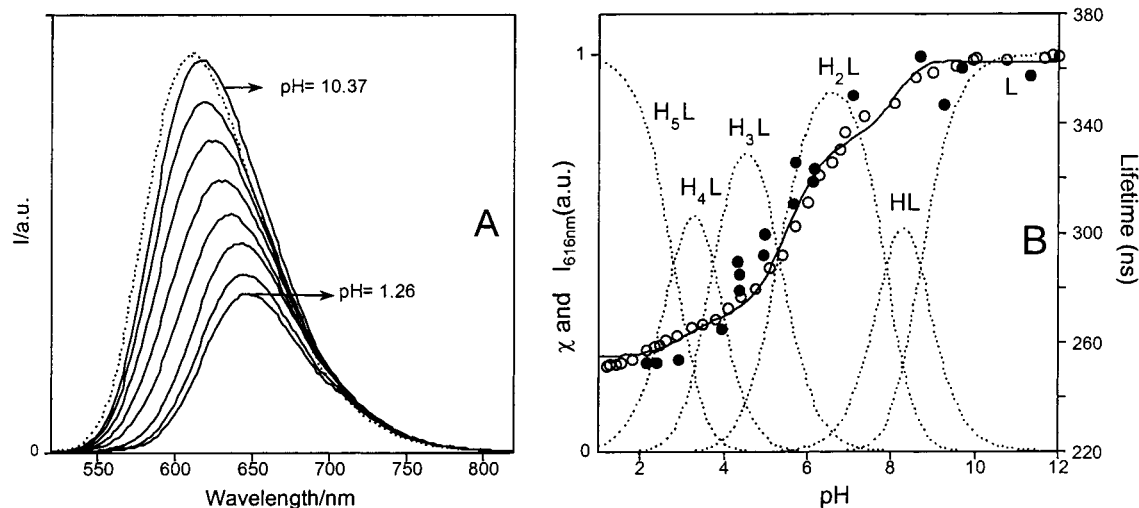


Figure 3. (A) Emission spectra of compound 2^{2+} (L) (—), 1.33×10^{-5} M, and $[\text{Ru}(\text{bpy})_3]\text{Cl}_2$, 1.33×10^{-5} M (---), as a function of pH. (B) (○) Emission titration curve obtained at $\lambda_{\text{em}} = 616$ nm and $\lambda_{\text{ex}} = 470$ nm; (●) lifetime titration curve, $\lambda_{\text{ex}} = 355$ nm; together with the representation of the mole fraction (χ) distribution of the protonated species. Charges omitted in species labels.

the coordinated Ru(II) ion. Nevertheless, highly charged species are formed in neutral and acidic solutions which may interact with anions, as discussed below.

The absorption spectrum of compound 2^{2+} at two different pH values is shown in Figure 2. It can be seen that the absorption spectra of compound 2^{2+} does not change significantly with pH, despite the observation of measurable modifications upon protonation of both benzylic nitrogens (H_4L^{2+} species); see inset of Figure 2. Moreover, the absorption spectrum of the nonprotonated species is practically identical to the one of the parent compound, $\text{Cl}_2[\text{Ru}(\text{bpy})_3]$. The small influence of the protonation stage of the receptor unit on the absorption characteristics of this type of signaling unit is in agreement with the results previously reported on compound **1**.^{4b}

At basic pH values ($\text{pH} > 10$), the emission of compound 2^{2+} is slightly red-shifted relative to the parent $[\text{Ru}(\text{bpy})_3]^{2+}$, and the obtained ratio of the quantum yields is $\Phi_2/\Phi_{[\text{Ru}(\text{bpy})_3]^{2+}} = 0.98$. In strong contrast with the absorption, the luminescence of compound 2^{2+} , shown in Figure 3, is affected by the pH of the medium. A large decrease of the emission is observed after the third (H_3L^{2+}) and fourth protonation steps (H_4L^{2+}) have occurred. The increase in protonation of the amino groups is followed by a significant red shift of ≈ 34 nm (from pH 10.37 to pH 1.26). It is interesting to note that an identical behavior was reported for compound **1**, but the decrease of intensity of emission is somewhat lower.^{4b} This effect can be explained by the fact that protonation of the receptor leads to a better electron acceptor, lowering the energy of the MLCT (metal–ligand charge transfer). An additional explanation can be found by considering that increasing protonation of the amino groups can gradually give rise to a more distorted state, which is in agreement with the observed increased Stokes shift. A more distorted excited-state geometry favors the radiationless processes, giving rise to a less emissive species, by decreasing the radiative rate constant. In Figure 3B, the luminescence lifetime dependence with pH exhibits a behavior identical to the one found for the titration curve built with luminescence quantum yields. This shows that compound 2^{2+} also behaves as a pH based lifetime chemosensor.

Sensing Zn(II). The stability constants potentiometrically determined for the complexes formed by 2^{2+} with Zn(II) are listed in Table 3. A comparison of these constants with those previously reported for **L**¹¹ indicates that, as could be expected,

Table 3. Zn²⁺ Complexation Constants with 2^{2+} Determined in 0.10 M Me₄NCl at 298.1 ± 0.1 K

reaction	log K
$\text{Zn}^{2+} + 2^{2+} = \text{Zn}2^{4+}$	8.06(7) ^a
$\text{Zn}2^{4+} + \text{H}^+ = \text{ZnH}2^{5+}$	7.13(7)
$\text{ZnH}2^{5+} + \text{H}^+ = \text{ZnH}_2\text{L}^{6+}$	6.10(9)
$\text{ZnH}_2\text{L}^{6+} + \text{H}^+ = \text{ZnH}_3\text{L}^{7+}$	5.03(6)
$\text{Zn}2^{4+} + \text{OH}^- = \text{Zn}2(\text{OH})^{3+}$	6.4(1)
$\text{Zn}2(\text{OH})^{3+} + \text{OH}^- = \text{Zn}2(\text{OH})_2^{2+}$	3.8(1)

^a Values in parentheses are standard deviations in the last significant figure.

L reduces its coordinating ability toward metal ions when its bipyridyl unit is linked to Ru(II). Nevertheless, 2^{2+} binds Zn(II) over all the pH range (2.5–11) investigated, giving rise to various protonated and hydroxylated species ranging from $[\text{Zn}(\text{H}_3\text{L})]^{7+}$ to $[\text{Zn}2(\text{OH})_2]^{2+}$.

The absorption, as well as the emission, of the Zn(II) complexes of compound 2^{2+} is only slightly red-shifted relative to the noncomplexed compound in the same pH range. The luminescence emission and lifetime based titration curves of compound 2^{2+} in the absence and in the presence of Zn(II) (1:1) (Figure S3, Supporting Information) show that Zn(II) coordination does not significantly change the intensity of the emission. Nevertheless, the $[\text{Zn}2]^{4+}$ species is slightly more emissive than the noncoordinated ligand, for the same pH values, and thus it is worthwhile to conclude that this ligand exhibits a modest detection ability for Zn(II).

Sensing Cu(II). In contrast with Zn(II), which forms only 1:1 complexes with 2^{2+} in solution, Cu(II) is also able to form 2:1 species. However, according to the stability constants determined for the Cu(II) complexes with 2^{2+} , and listed in Table 4, the ligand does not display a great tendency to bind the second Cu(II) ion, and for this reason only 1:1 complex species are formed in solution containing 2^{2+} and metal ion in 1:1 molar ratio. Distribution diagrams (Figure S4) of the complexes formed in solution are reported within the Supporting Information.

The absorption spectrum of 2^{2+} is only slightly affected, in terms of shift and shape, by Cu(II) complexation. However, contrasting with the previous Zn(II) complexes, the emission in the presence of Cu(II) ion shows a dramatic quenching upon coordination to the metal (Figure 4) and, very surprisingly, for high pH values the emission is restored and a new band appears in the high energy region of the spectrum (blue shift of 28

Table 4. Cu^{2+} Complexation Constants with 2^{2+} Determined in 0.10 M Me_4NCl at 298.1 ± 0.1 K

reaction	log K
$\text{Cu}^{2+} + 2^{2+} = \text{Cu}2^{4+}$	14.1(1) ^a
$\text{Cu}2^{4+} + \text{H}^+ = \text{CuH}2^{5+}$	6.33(7)
$\text{CuH}2^{5+} + \text{H}^+ = \text{CuH}_22^{6+}$	5.11(4)
$\text{Cu}2^{4+} + \text{OH}^- = \text{Cu}2(\text{OH})^{3+}$	3.8(1)
$\text{Cu}2^{4+} + \text{Cu}^{2+} = \text{Cu}_22^{6+}$	3.7(2)
$\text{Cu}_22^{6+} + \text{OH}^- = \text{Cu}_22(\text{OH})^{5+}$	8.1(1)
$\text{Cu}_22(\text{OH})^{5+} + \text{OH}^- = \text{Cu}_22(\text{OH})_2^{4+}$	5.2(1)

^a Values in parentheses are standard deviations in the last significant figure.

nm). Moreover, the lifetime at these pH values is reduced to ca. 0.5 ns.

The quenching of the emission of $[\text{Ru}(\text{bpy})_3]^{2+}$ by polyamine complexes of $\text{Cu}(\text{II})$ ion was previously described by Moore and Alcock and attributed to energy transfer from the excited state of $[\text{Ru}(\text{bpy})_3]^{2+}$ to the copper complex, promoting a d–d transition of $\text{Cu}(\text{II})$.⁶ On the other hand, it is not possible to give a sure interpretation of the lack of quenching effect and the consequent increase of emission observed at very high pH values ($\text{pH} > 11$), since this pH range ($\text{pH} > 11$) is outside the pH windows useful for our potentiometric measurements. Consequently, we were not able to perform the speciation of the system under such conditions. However, it seems most likely that the revival of the emission in very alkaline solution may be due to the formation of $\text{Cu}(\text{II})$ hydroxo complexes, determining the stripping of the metal ion from the macrocyclic cavity. Indeed, calculations²³ performed by using the stability constants reported in Table 4 for the copper(II) complexes of 2^{2+} , the stability constants²⁴ of the $\text{Cu}(\text{II})$ hydroxo complexes (from $[\text{Cu}(\text{OH})]^+$ to $[\text{Cu}(\text{OH})_4]^{2-}$), and the solubility product²⁴ of copper(II) hydroxide indicate that, under the experimental conditions of the photochemical measurements, formation of the $\text{Cu}(\text{II})$ hydroxo complexes would take place according to the profile of the increasing emission in alkaline solutions. Support for this interpretation is provided by the fact the emission spectra obtained, in alkaline media, in the presence of $\text{Cu}(\text{II})$ (Figure 4) are consistent with those obtained under the same conditions for compound 2^{2+} in the absence of metal ion (Figure 3).

Sensing Metalloacyanide Complex Anions. It is well-known that macrocyclic polyamines in their protonated forms are efficient receptors of anionic species in solution.²⁵ In particular, very stable adducts are formed with $[\text{Fe}(\text{CN})_6]^{4-}$ and $[\text{Fe}(\text{CN})_6]^{3-}$, principally due to the high negative charge of such anions.^{26–28} Hence, we expected that also protonated species of 2^{2+} might be able to form similar adducts. Our principal interest in such systems stems from the fact that the emission of the parent compound $[\text{Ru}(\text{bpy})_3]^{2+}$ is known to be efficiently quenched by electron transfer from (or to) metalloacyanide complexes,^{29–31}

and thus $[\text{Ru}(\text{bpy})_3]^{2+}$ could be used as a sensor for this type of anion. Compound 2^{2+} contains the basic ruthenium sensing unit, but in addition possesses an extra binding polyamine receptor that is expected to influence the overall process, improving the efficiency in anion sensing. In the forthcoming presentation and discussion of data, we will analyze the system and compare the performances of compound 2^{2+} with the parent compound $[\text{Ru}(\text{bpy})_3]^{2+}$.

The interaction of 2^{2+} with $[\text{Fe}(\text{CN})_6]^{4-}$ was studied by means of potentiometric measurements, which furnished the speciation of the systems, and the equilibrium constants of the species formed (Table 5). As shown by Figure 5, anion complexes $\{\text{H}_n2[\text{Fe}(\text{CN})_6]\}^{(n-2)+}$ with increasing protonation degree ($n = 2–5$) are formed on lowering the solution pH. As generally observed for this type of complex, their thermodynamic stability increases with increasing ligand protonation (Table 5), evidencing the major contribution given by electrostatic forces to the anion–receptor pairing. Accordingly, the equilibrium constant for the interaction of H_42^{6+} with $[\text{Fe}(\text{CN})_6]^{4-}$ is significantly higher than that found for the interaction of the same ligand species with the less charged form $[\text{HFe}(\text{CN})_6]^{3-}$ (Table 5). The formation of hydrogen bonds between the protonated polyamine moiety of the receptor and the anion, as observed for perchlorate in the crystal structure of $(\text{H}_32)(\text{ClO}_4)_5 \cdot \text{H}_2\text{O}$, is expected to further stabilize the anion complex in solution.

As expected, the emission of compound 2^{2+} is very efficiently quenched by interaction with $[\text{Fe}(\text{CN})_6]^{4-}$ and $[\text{Fe}(\text{CN})_6]^{3-}$. These quenching processes may have contributions from adducts already present in the ground state (static quenching) or formed during the excited-state lifetime of the emissive species (dynamic quenching). Such contributions can be separated if lifetime measurements are carried out in parallel with steady-state fluorimetric measurements (see Supporting Information).

The Stern–Volmer plots (see Supporting Information) for the adducts involving $[\text{Ru}(\text{bpy})_3]^{2+}$ and H_42^{6+} , respectively, at pH 4.0 with $[\text{Fe}(\text{CN})_6]^{4-}$ as well as with $[\text{Fe}(\text{CN})_6]^{3-}$ showed an upward curvature of I_0/I in comparison with τ_0/τ , indicating the existence of ion-pair association in the ground state. These systems were treated to take into account both static and dynamic quenching, the resulting constants being reported in Table 6. The association is negligible for the pair between $[\text{Ru}(\text{bpy})_3]^{2+}$ and $[\text{Fe}(\text{CN})_6]^{3-}$. In the case of the pair $[\text{Ru}(\text{bpy})_3]^{2+}$ and $[\text{Fe}(\text{CN})_6]^{4-}$, I_0/I is somewhat higher than τ_0/τ , allowing calculation of an association constant $K_{\text{ip}} < 300$. On the other hand, the quenching constants for the dynamic quenching, K_{SV} , are comparable with those reported by Balzani et al.²⁹ The observed differences can be attributed to the differences in ionic strength used by these authors.

As reported previously,^{29,30} the mechanism responsible for the observed quenching in the systems involving $[\text{Ru}(\text{bpy})_3]^{2+}$ and the iron complexes is due to electron transfer from the excited $\text{Ru}(\text{II})$ complex to the $\text{Fe}(\text{III})$ complex, and vice versa from the $\text{Fe}(\text{II})$ complex to the excited $\text{Ru}(\text{II})$.

The effect of the polyamine chain of 2^{2+} , in both ion-pair-association constant and dynamic quenching, was studied at pH 4. At this pH value, and in the presence of fluorophore concentration of about 1×10^{-5} M, four of the five nitrogens of the polyamine macrocycle are protonated. In both systems

- (23) *Hys* computer program. Alderighi, L.; Gans, P.; Ienco, A.; Peters, D.; Sabatini, A.; Vacca, A. *Coord. Chem. Rev.* **1999**, *184*, 311.
- (24) Smith, R. M.; Martell, A. E. *NIST Critical Stability Constants Database*, version 2; National Institute of Standards and Technology: Washington, DC, 1995.
- (25) *Supramolecular Chemistry of Anions*; Bianchi, A., Bowman-James, K., Garcia-España, E., Eds.; Wiley-VCH: New York, 1997.
- (26) Peter, F.; Gross, M.; Hosseini, M. W.; Lehn, J.-M.; Sessions, R. B. *J. Chem. Soc., Chem. Commun.* **1981**, 1067. Peter, F.; Gross, M.; Hosseini, M. W.; Lehn, J.-M. *Electroanal. Chem.* **1983**, *144*, 279.
- (27) Garcia-España, E.; Micheloni, M.; Paoletti, P.; Bianchi, A. *Inorg. Chim. Acta* **1985**, *102*, L9. Bencini, A.; Bianchi, A.; Garcia-España, E.; Giusti, M.; Mangani, S.; Micheloni, M.; Orioli, P.; Paoletti, P. *Inorg. Chem.* **1987**, *26*, 3902. Aragón, J.; Bencini, A.; Bianchi, A.; Domenech, A.; Garcia-España, E. *J. Chem. Soc., Dalton Trans.* **1992**, 319.
- (28) Bianchi, A.; Domenech, A.; Garcia-España, E.; Luis, S. *Anal. Chem.* **1993**, *65*, 3137.

- (29) Juris, A.; Gandolfi, M. T.; Manfrin, M. F.; Balzani, V. *J. Am. Chem. Soc.* **1976**, *98*, 1047.
- (30) Mallouk, T. E.; Krueger, J. S.; Mayer, J. E.; Dymond, C. M. G. *Inorg. Chem.* **1989**, *28*, 3507.
- (31) Roundhill, D. M. *Photochemistry and Photophysics of Metal Complexes*; Plenum Press: New York, 1994.

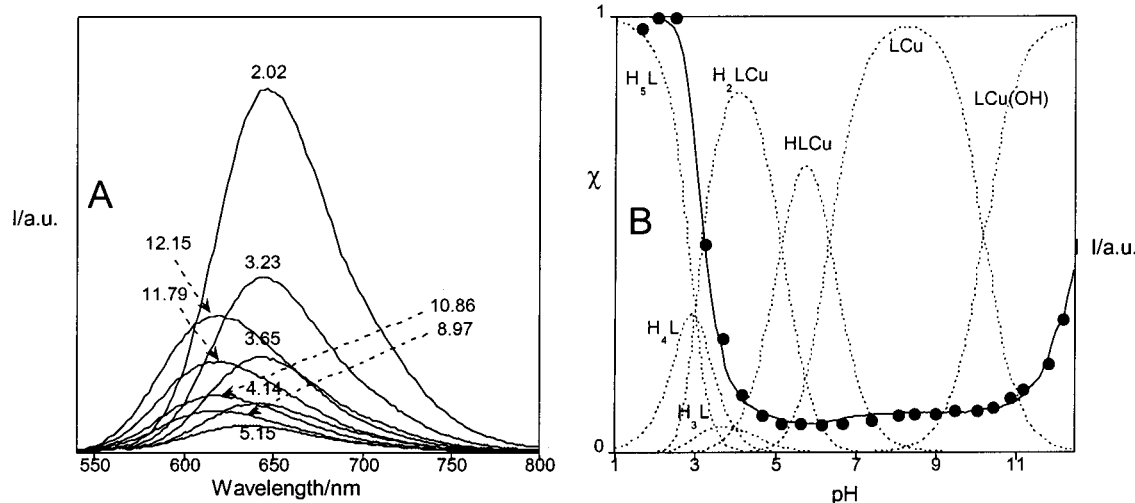


Figure 4. (A) pH-dependent emission spectra of compound 2^{2+} (L), 1.33×10^{-5} M, in the presence of equimolar concentration of Cu^{2+} . (B) (●) Emission intensity titration curve obtained at $\lambda_{\text{em}} = 616$ nm and $\lambda_{\text{ex}} = 470$ nm. Solid lines are mole fraction (χ) distribution curves of the species present in solution (charges omitted). Charges omitted in species labels.

Table 5. $[\text{Fe}(\text{CN})_6]^{4-}$ Complexation Constants with 2^{2+} Determined in 0.10 M Me_4NCl at 298.1 ± 0.1 K

reaction	log K
$[\text{Fe}(\text{CN})_6]^{4-} + \text{H}_2\text{2}^{4+} = \text{H}_2[\text{Fe}(\text{CN})_6]$	4.48(7) ^a
$[\text{Fe}(\text{CN})_6]^{4-} + \text{H}_3\text{2}^{5+} = \{\text{H}_3\text{2}[\text{Fe}(\text{CN})_6]\}^+$	5.70(6)
$[\text{Fe}(\text{CN})_6]^{4-} + \text{H}_4\text{2}^{6+} = \{\text{H}_4\text{2}[\text{Fe}(\text{CN})_6]\}^{2+}$	6.67(6)
$[\text{HFe}(\text{CN})_6]^{3-} + \text{H}_4\text{2}^{6+} = \{\text{H}_5\text{2}[\text{Fe}(\text{CN})_6]\}^{3+}$	5.97(7)

^a Values in parentheses are standard deviations in the last significant figure.

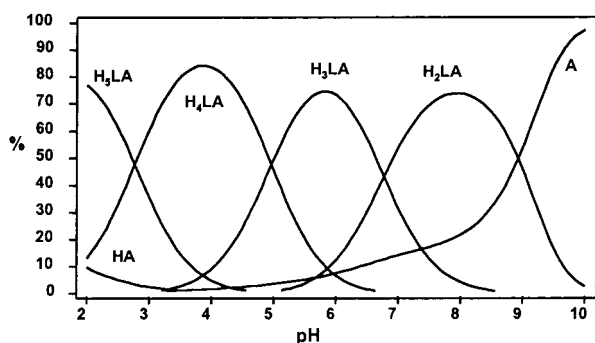


Figure 5. Distribution curves of anion complexes formed by compound 2^{2+} with $[\text{Fe}(\text{CN})_6]^{4-}$ in aqueous solution. Charges omitted in species labels.

Table 6. Association Constants (log K_{ip}) and Quenching Rate Constants (k_{q}) Determined from Photophysical Quenching Studies

	log K_{ip}^a	$K_{\text{SV}}^a/\text{M}^{-1}$	$K_{\text{SV}}^b/\text{M}^{-1}$	$k_{\text{q}}/\text{s}^{-1} \text{M}^{-1}$
$[\text{Fe}(\text{CN})_6]^{4-} + [\text{Ru}(\text{bpy})_3]^{2+}$	2.5	2325	1320	5.8×10^9 ^c
$[\text{Fe}(\text{CN})_6]^{3-} + [\text{Ru}(\text{bpy})_3]^{2+}$		3488	2600	8.7×10^9 ^c
$[\text{Fe}(\text{CN})_6]^{4-} + [\text{Ru}(\text{bpy})_2(\text{H}_4\text{L})]^{6+}$	4.7	4164		1.4×10^{10} ^d
$[\text{Fe}(\text{CN})_6]^{3-} + [\text{Ru}(\text{bpy})_2(\text{H}_4\text{L})]^{6+}$	3.3	3697		1.3×10^{10} ^d

^a All experiments were carried out at 298 K, in air atmosphere, at pH 4.0. ^b Values from ref 27. ^c $\tau_0([\text{Ru}(\text{bpy})_3]^{2+}) = 400$ ns. ^d $\tau_0([\text{Ru}(\text{bpy})_2(\text{H}_4\text{L})]^{6+}) = 290$ ns.

$(\text{H}_4\text{2}^{6+}/[\text{Fe}(\text{CN})_6]^{4-}$ and $\text{H}_4\text{2}^{6+}/[\text{Fe}(\text{CN})_6]^{3-}$) the ion-pair association dominates the interaction. This is due to the increase of the charge in the ruthenium complex from 2+ to 6+, and to the formation of hydrogen bonding between the protonated

nitrogens of the host and the cyanide ligands of the guest. As expected, the ion-pair association is stronger for $[\text{Fe}(\text{CN})_6]^{4-}$ than for $[\text{Fe}(\text{CN})_6]^{3-}$, because of the larger charge in the former. The ion-pair-association constants obtained for the $\text{H}_4\text{2}^{6+}$ and $[\text{Fe}(\text{CN})_6]^{4-}$ (log $K_{\text{ip}} = 4.7$) system is lower than the values obtained by potentiometry (log $K_{\text{ip}} = 6.7$). This difference can be attributed to the larger influence of the chloride ions from the medium ($[\text{Cl}^-] = 0.10$ M) in the case of the fluorimetric measurements ($[\text{H}_4\text{2}^{6+}] = 1.0 \times 10^{-5}$ M), compared with the potentiometric experiments ($[\text{H}_4\text{2}^{6+}] = 1.0 \times 10^{-3}$ M).

Regarding the dynamic quenching, the association constants (Table 6) are similar for both adducts and the respective rates (Table 6) seem to indicate that these are controlled by diffusion processes. The small increase of the quenching rate constant from the adducts involving $[\text{Fe}(\text{CN})_6]^{3-}$ to those with $[\text{Fe}(\text{CN})_6]^{4-}$ can be attributed to an increase of the driving force for complex formation, determined by the increasing anion charge.

Our systems involve electron transfer through hydrogen bonds between charged species. They have, thus, some resemblance to the systems studied by Harriman and Sessler,¹⁰ and by Nocera,^{9b,d} in which energy/electron transfer in cytosine/guanine H-bonded assemblies and guanidinium/carboxylate salt bridges were studied, respectively. These studies showed that both types of bridges influence the rate constants for the energy/electron transfer and it cannot be excluded that some kind of mediation involving the hydrogen bonds between the cyanide groups of $[\text{Fe}(\text{CN})_6]^{4-}$ and the ammonium groups of $\text{H}_4\text{2}^{6+}$ may be present in our systems. However, within the time resolution of our equipment (ca. 10 ns), only monoexponential decays were observed, which prevented the determination of the photoinduced electron transfer rate constants.

Figure 6 shows the variation of the $E_{1/2}$ for the iron complex, as a function of the molar ratio $\text{H}_4\text{2}^{6+}/[\text{Fe}(\text{CN})_6]^{4-}$ obtained by cyclic voltammetry at a constant concentration of $\text{H}_4\text{2}^{6+}$ (1×10^{-3} M) in 0.10 M NaCl at pH 4. As reported previously, the shift of $E_{1/2}$ before and after complexation (ΔE) is related to the ratio of the ion-pair-association constants of both reduced and oxidized iron complexes with $\text{H}_4\text{2}^{6+}$, by eq 1:²⁸

$$\Delta E = \frac{RT}{nF} \ln \frac{K_{\text{ip}}(\text{red})}{K_{\text{ip}}(\text{ox})} \quad (1)$$

This equation was used to calculate log $K_{\text{ip}}(\text{ox}) = 5.3$ between

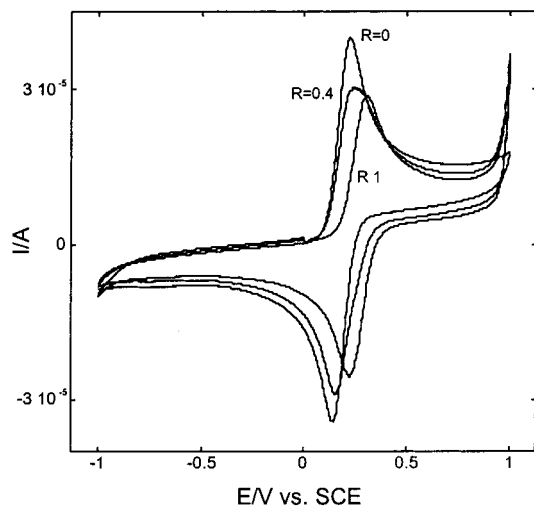


Figure 6. Cyclic voltammetry of $[\text{Fe}(\text{CN})_6]^{4-}$ 1×10^{-3} M, in 0.1 M NaCl at pH 4.0 as a function of addition of $\text{H}_4\text{2}^{6+}$; $R = \text{H}_4\text{2}^{6+}/[\text{Fe}(\text{CN})_6]^{4-}$

$\text{H}_4\text{2}^{6+}$ and $[\text{Fe}(\text{CN})_6]^{3-}$, using $\log K_{\text{ip}}(\text{red}) = 6.7$ obtained from potentiometry carried out under the same conditions as those of the voltammetry experiments. This value is larger than the one obtained by fluorimetry ($\log K_{\text{ip}} = 3.3$) for the reasons described above, i.e., the influence of the chloride ion.

The results reported above show that the presence of the polyamine chain increases the performance of 2^{2+} in sensing the two iron cyanide complexes when compared with the parent compound $[\text{Ru}(\text{bpy})_3]^{2+}$.

Iodide to Iodine Photocatalytic Oxidation. Aqueous solutions of 2^{2+} (1.55×10^{-4} M), in the presence of 0.1 M sodium iodide, lead to the formation of a precipitate. For this reason a (9:1) water/acetonitrile mixture, at pH 4.3, was used to increase the solubility. The absorption spectrum of such solution is the summation of the spectra of both components, and thus there is no evidence for the formation of ion-pair charge transfer. However, the fluorescence emission of compound 2^{2+} is quenched by about 5% in the presence of $[\text{I}^-] = 0.1$ M. In the case of the parent compound $[\text{Ru}(\text{bpy})_3]^{2+}$, its fluorescence is not affected by addition of the same amount of iodide. When air-equilibrated solutions of 2^{2+} in the presence of $[\text{I}^-] = 0.1$ M, at pH 4.3, are irradiated at 436 nm, formation of I_3^- is immediately observed by the increasing of its characteristic absorption band centered at 350 nm. The quantum yield of this photoreaction, based on the total amount of light absorbed by the system, is 0.0033. Taking into account that only 5% of the emission of compound 2^{2+} is quenched by the iodide, the true quantum yield is ca. 0.07.

If nitrogen is bubbled in the same solution before irradiation, no steady-state spectral modifications can be observed. On the contrary, saturation of the solutions with dioxygen increases the quantum yield by ca. 5-fold. It is interesting to note that no spectral variations were detected in the absorption spectrum of the parent compound $[\text{Ru}(\text{bpy})_3]^{2+}$ irradiated in the presence of $[\text{I}^-] = 0.1$ M.

Formation of iodine by photocatalytic oxidation of iodide is a well-established reaction reported for some other systems, namely for the case of the ion pairs involving iodide and $\text{Co}(\text{sep})^{3+}$ ($\text{sep} = \text{sepulchrate} = 1,3,6,8,10,13,16,19\text{-octaazabicyclo-[6.6.6]eicosane}$).³² The experimental results can be accounted for by Figure 7. Excitation of compound 2^{2+} in the MLCT band allows the transfer of one electron from I^- to the Ru(II) complex, leading to the formation of an iodine radical and to a Ru(II)

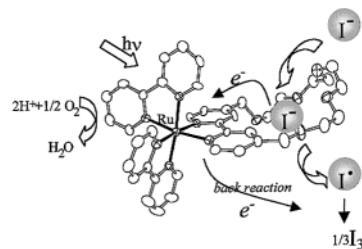
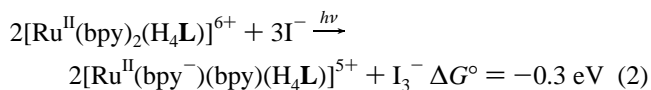


Figure 7. Photocatalytic cycle for the oxidation of iodide to iodine by dioxygen.

complex with a reduced dipyrindine radical anion. The iodine radical gives I_3^- as a final product by a sequence of well-known reactions.³² The cycle is completed by reoxidation of the dipyrindine radical by dioxygen.

As demonstrated by the inertness of the parent $[\text{Ru}(\text{bpy})_3]^{2+}$ compound, the existence of the positively charged macrocyclic receptor seems to be an indispensable requirement to fix the iodide in a position close to the metal, to allow the electron transfer process. In the case of $\text{H}_4\text{2}^{6+}$, the net reaction can be accounted for by eq 2, which is thermodynamically favorable by 0.3 eV.



The relatively low efficiency of this system (0.35 in dioxygen saturated solutions) can be attributed to the fact that only 5% of the excited state can be quenched by iodide. In addition there is evidence, from preliminary flash photolysis experiments, that the back reaction from the reduced complex to I_3^- is a competitive process that decreases the net formation of photo-products.

Conclusions

Macrocycles containing endotopic cavities and exotopic coordination sites can be used as ligands in the construction of water-soluble fluorescent metal complexes. These coordination compounds can be used as luminescence chemosensors based on the emission intensity, as well as in long-lifetime-based sensing for cations and anions. In addition, the receptor cavity can be explored as a photocatalytic center capable of hosting substrates amenable to reaction upon electron or energy transfer involving the metal center.

Acknowledgment. This work has been supported by the Ministero dell'Università e della Ricerca Scientifica e Tecnologica (MURST, Rome) within the program COFIN 2000.

Supporting Information Available: A X-ray crystallographic file for $(\text{H}_3\text{2})(\text{ClO}_4)_5 \cdot \text{H}_2\text{O}$, in CIF format, is available on the Internet only. Description of the crystal packing with ORTEP representations (Figures S1 and S2) and hydrogen bond contacts (Table S1). Luminescence emission and lifetime based titration curves of compound 2^{2+} in the presence of Zn(II) (Figure S3). Distribution curves of Cu(II) complexes formed by compound 2^{2+} (Figure S4). Stern–Volmer plots (Figure S5) with description. This material is available free of charge via the Internet at <http://pubs.acs.org>.

IC0105213

(32) (a) Pina, F.; Ciano, M.; Moggi, L.; Balzani, V. *Inorg. Chem.* **1985**, *24*, 844. (b) Pina, F.; Maestri, M.; Ballardini, R.; Mulazzani, Q. G.; D'Angelantonio, M.; Balzani, V. *Inorg. Chem.* **1986**, *25*, 4249. (c) Pina, F.; Sotomayor, J.; Moggi, L. *J. Photochem. Photobiol. A* **1990**, *53*, 411.